Supplementary Material

Ethan Lee[1*], Neil Ross[1], Andrew C. G. Henderson[1], Andrew J. Russell[1], Stewart S. R. Jamieson[2], Derek Fabel[3]

*** Correspondence:**
Ethan Lee (e.lee5@newcastle.ac.uk)

Data availability

The original data generated within this study can be found in the data.ncl repository at DOI: https://doi.org/10.25405/data.ncl.19307591 (Lee et al., 2022). Pléiades and SPOT 6/7 imagery used within this study are not readily available due to data belongs to third parties. The original data generated within this study include:

Geomorphological features:

- Alluvial fan
- Alluvial plain
- Bedrock step
- Boulders
- Cirque
- Glacial lineations
- Hill slope failures
- Hummocky terrain
- Moraines
- Moraine deposits
- Palaeo hill slope failures
- Pronounced moraine crests
- Rivers/streams
- Smoothed bedrock
- Steep bedrock slopes
- Waterbodies

Glacier reconstructions:

- Reconstructed glacier outlines with metrics
- Reconstructed glacier ELAs
- Reconstructed glacier profile contours

Basemap data:

- Streams/rivers
- 200 m contours
- Study regions
- Height points

Supplementary Table 1. Summary of remotely sensed data used for geomorphological mapping of the Las Huaringas region.

Satellite	Image ID	Date Acquired	Cloud Cover
Landsat 8	LC08_L1TP_010063_20161120_20200905_02_T1	20/11/16	5.4%
Sentinel-2	L1C_T17MPQ_A003669_20171118T153646	18/11/17	2.5%
RapidEye	20200106_151210_1736721_RapidEye-3	06/01/20	3%
RapidEye	20200106_151209_1736722_RapidEye-3	06/01/20	0%
RapidEye	20200106_151206_1736821_RapidEye-3	06/01/20	0%
RapidEye	20200106_151206_1736822_RapidEye-3	06/01/20	0%
PlanetScope	20200528_145133_93_2304	28/05/20	0%
PlanetScope	20200528_145136_32_2304	28/05/20	0%
PlanetScope	20200528_145138_72_2304	28/05/20	1%
Pléiades	DS_PHR1B_201512041554053_PS1_PX_W080S06_0624_02618	04/12/15	4.5%
Pléiades	DS_PHR1B_201801031552304_FR1_PX_W080S06_0618_03920	03/01/18	0.6%
Pléiades	DS_PHR1B_201911171547555_FR1_PX_W080S05_0802_01804	17/11/19	7.5%
Bing Maps[a]	NA	NA	~0%
Google Earth™[a]	NA	NA	~0%
ALOS DEM[b]	ALPSMLC30 v3.1	06/20	NA
SPOT 7[c]	DS_SPOT7_202005111517362_FR1_FR1_SV1_SV1_W079S05_01140	11/05/20	20.9%

[a] Bing Maps and Google Earth™ imagery are from multiple sources, cloud cover estimated upon manual inspection
[b] The ALOS DEM is generated from images from the JAXA ALOS collected between 2006 – 2011
[c] Captured in tri-stereo producing three images, but the image ID represents the entire collection

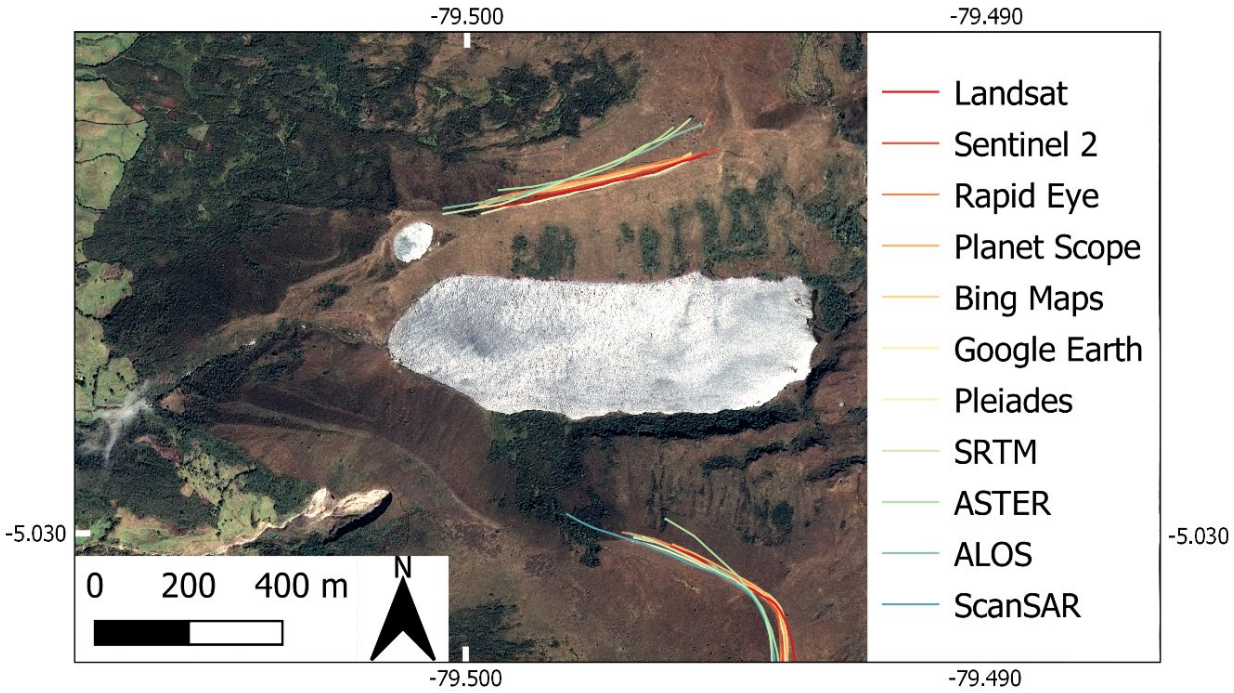

Supplementary Figure 1. Two digitized moraine crests around the L. la Cruz, within the western glacial cirques, using different remotely sensed sources. These are ordered in the legend with remotely sensed imagery sources from coarsest to finest resolution (Landsat 30 m to Pléiades 0.5 m), and DEM sources from coarsest to finest resolution (SRTM 30 m to ScanSAR 18 m). Maximum off set between the two mapped moraines was ± 30 m. Base image is Pléiades imagery.

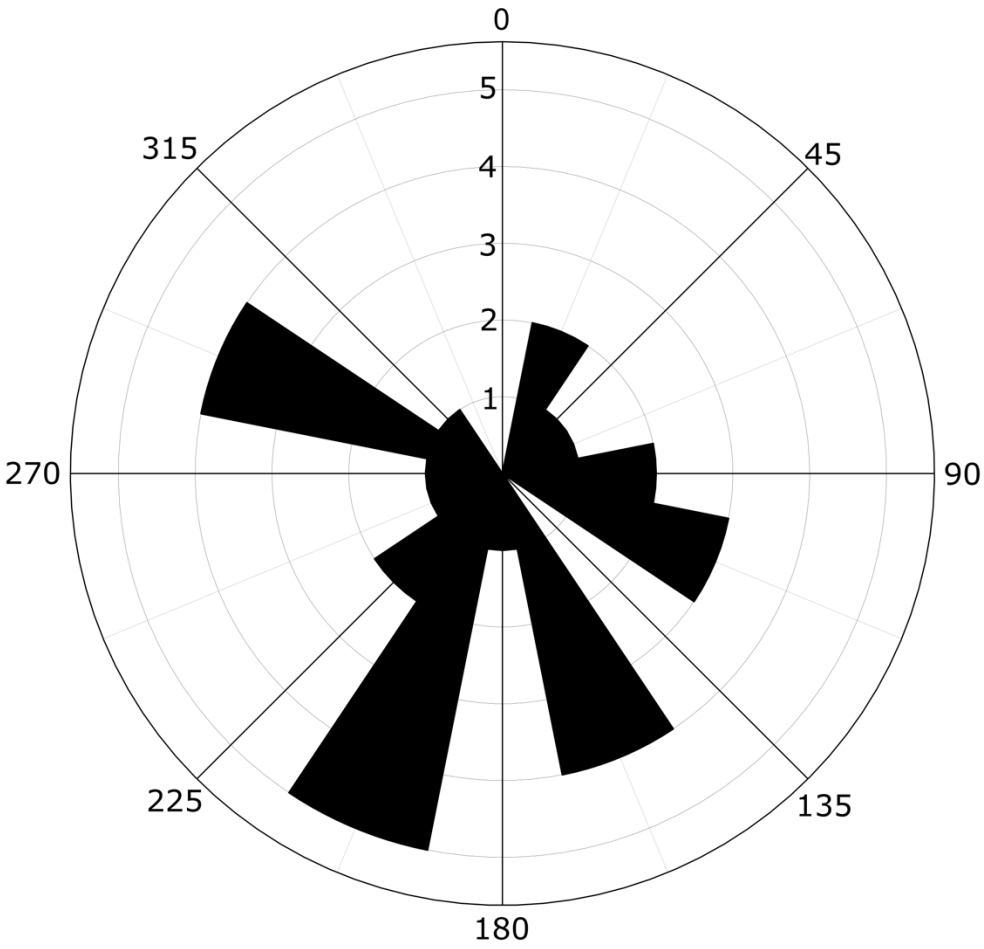

Supplemental Figure 2. Reconstructed palaeoglacier aspects that were manually delineated by digitizing a line from the head of the glacier towards the terminus, showing that the majority of the reconstructed glaciers face south (SE and SW).

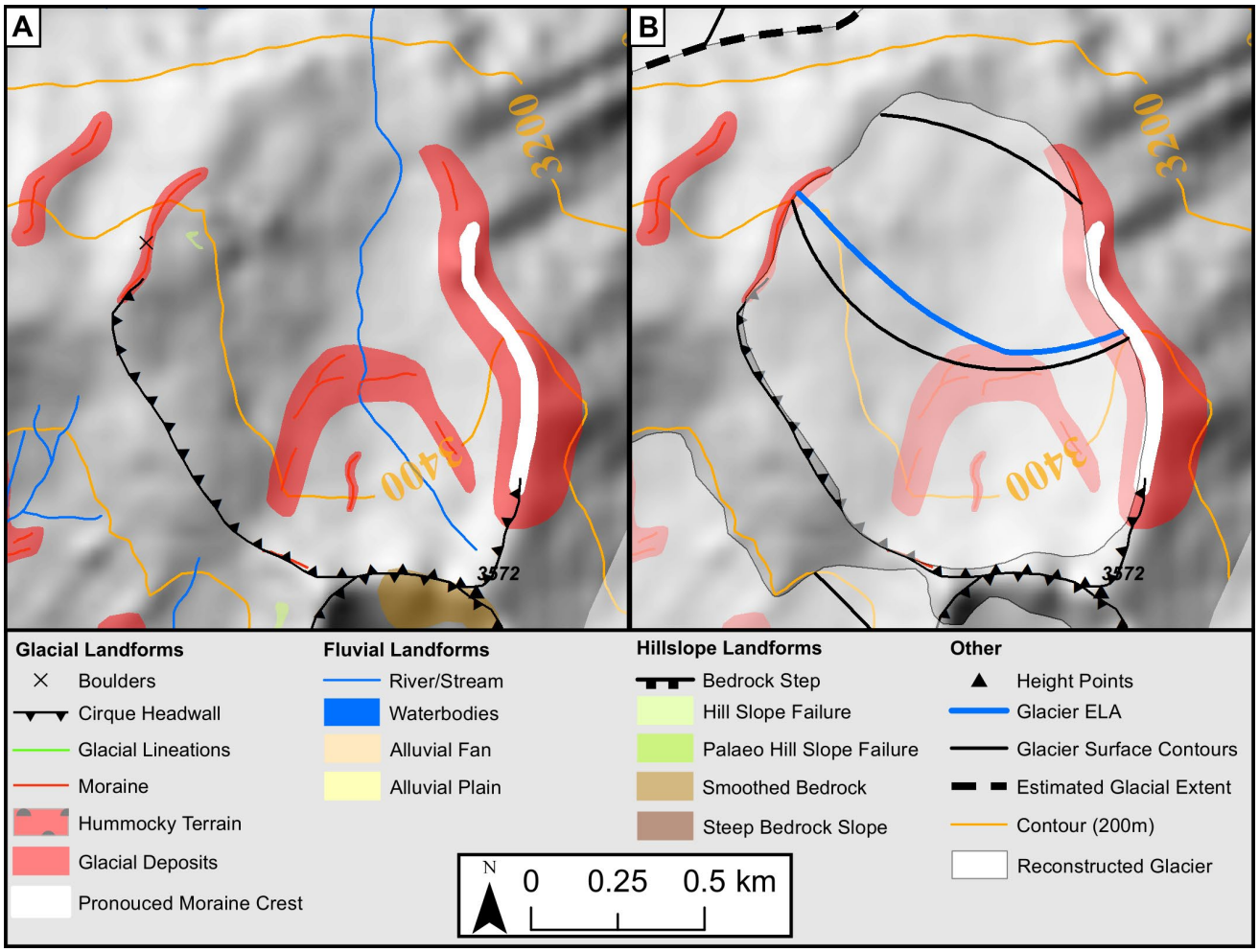

Supplementary Figure 3. Zoom in of the Quebrada Los Rosarios 1 glacier corresponding to Figure 8 B subset 1 with A) mapped geomorphology and B) the subsequent reconstructed LLGM glacier extent. Base map is a hillshade from the ALOS 30 m DEM.

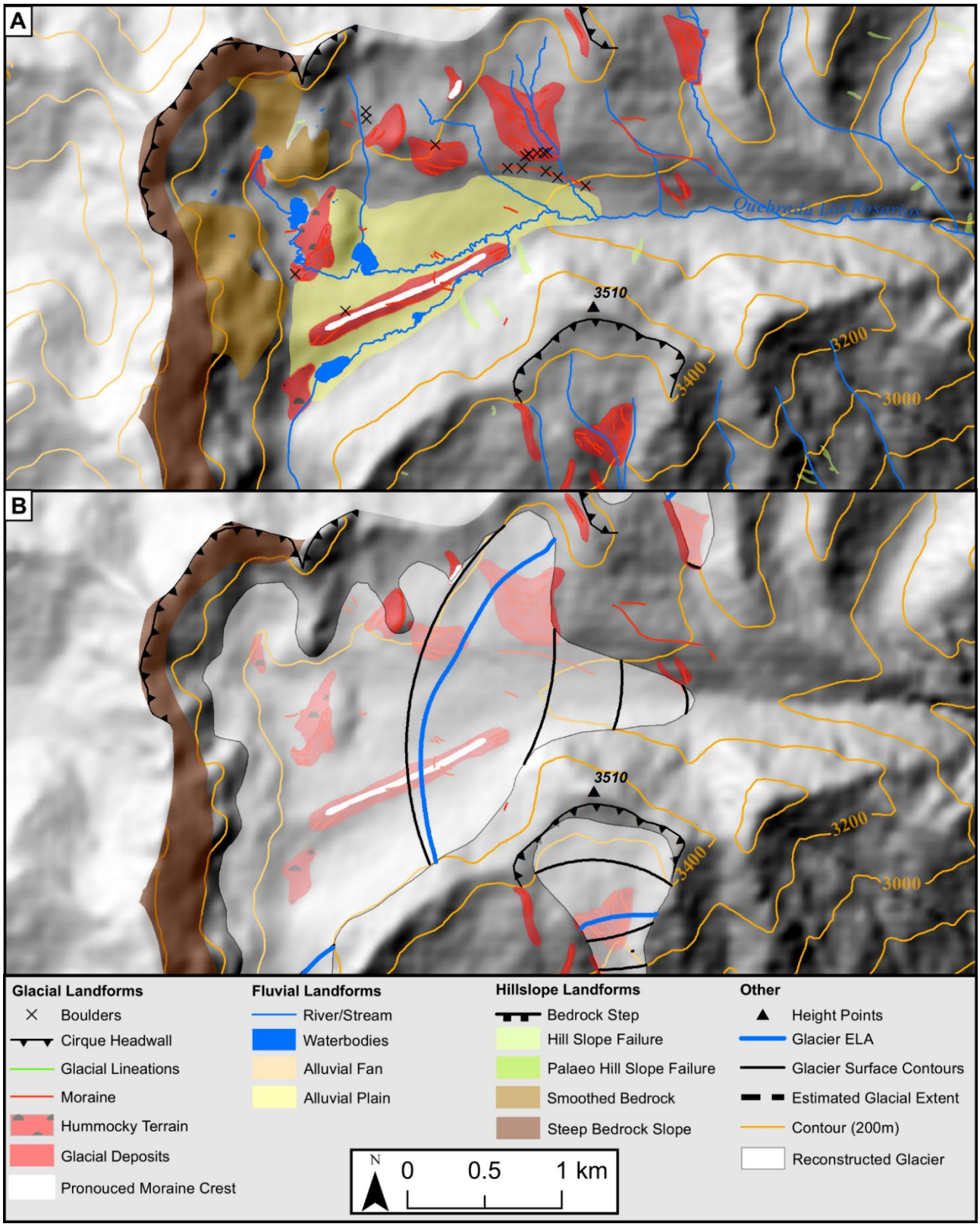

Supplementary Figure 4. Zoom in on the northern section of the Huancabamba 1 glacier corresponding with Figure 8 B subset 2 with A) mapped geomorphology and B) the subsequent reconstructed LLGM glacier extent. Base map is a hillshade from the ALOS 30 m DEM.

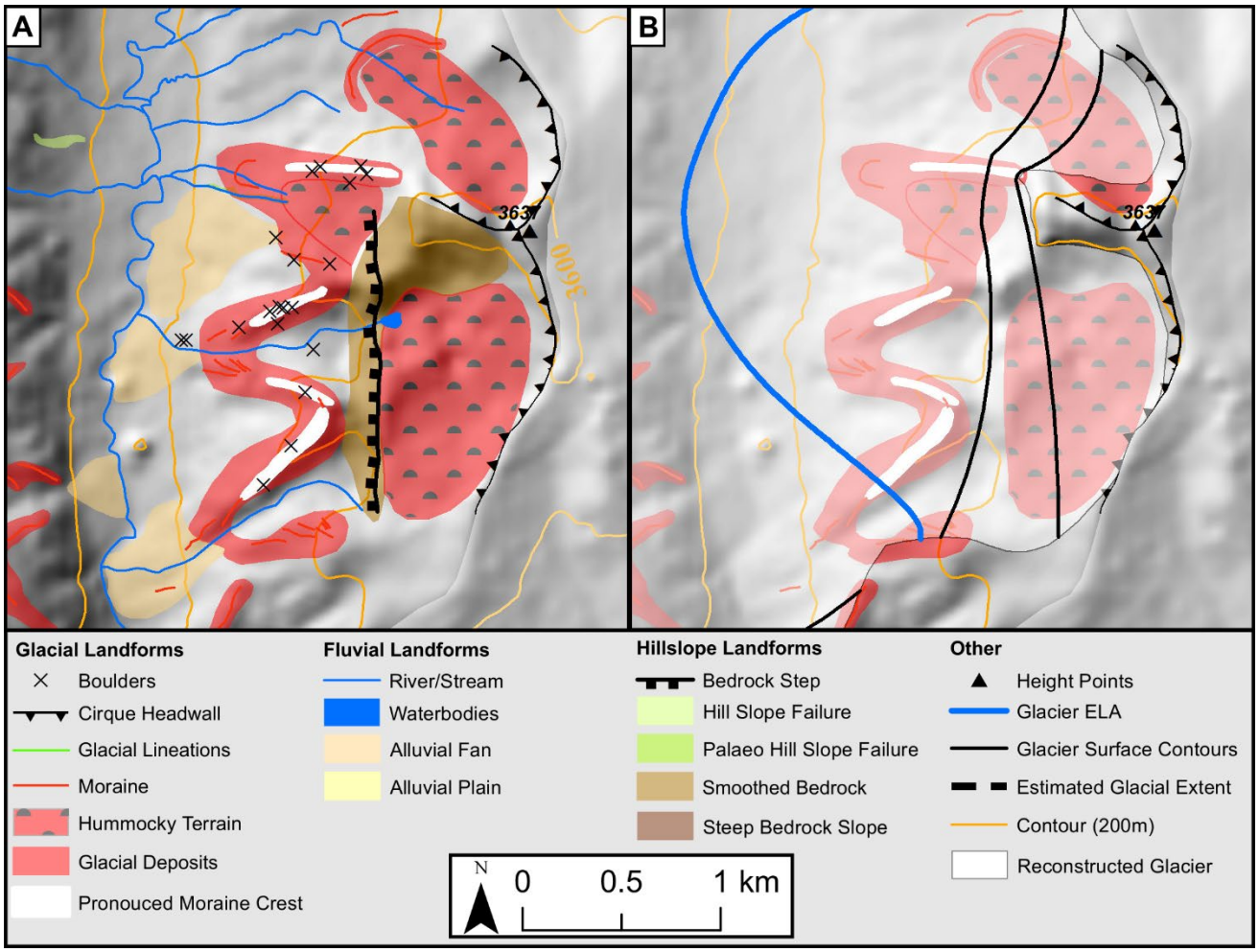

Supplementary Figure 5. Zoom in of the three glacial outlets in the southern section of the Huancabamba glacier, corresponding with Figure 8 B subset 3 with A) mapped geomorphology and B) the subsequent reconstructed glacier LLGM extent. Base map is a hillshade from the ALOS 30 m DEM.

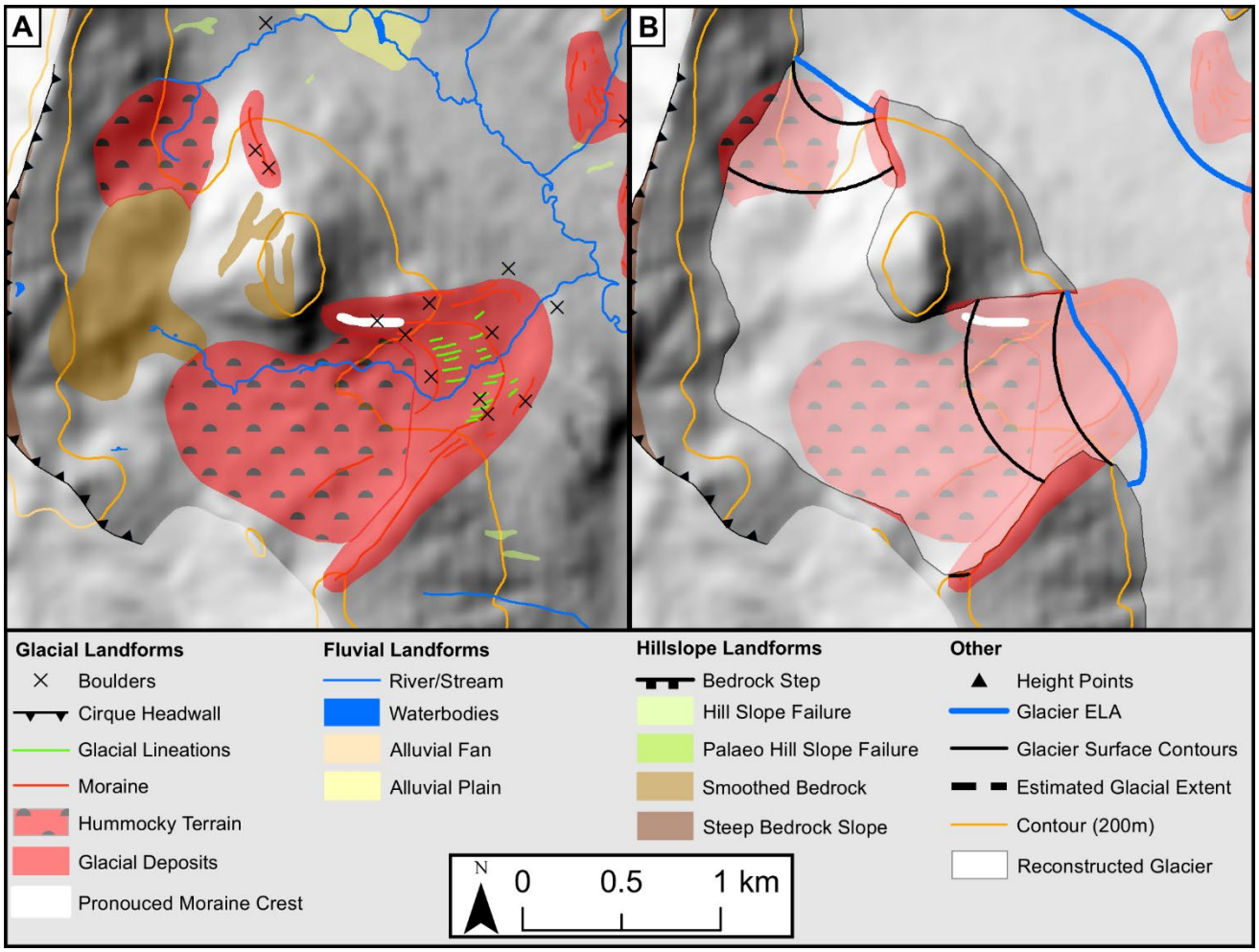

Supplementary Figure 6. Zoom in of the western outlet in the southern section of the Huancabamba glacier with two outlets and the glacier lineations, corresponding with Figure 8 B subset 4 with A) mapped geomorphology and B) the subsequent reconstructed glacier LLGM extent. Base map is a hillshade from the ALOS 30 m DEM.

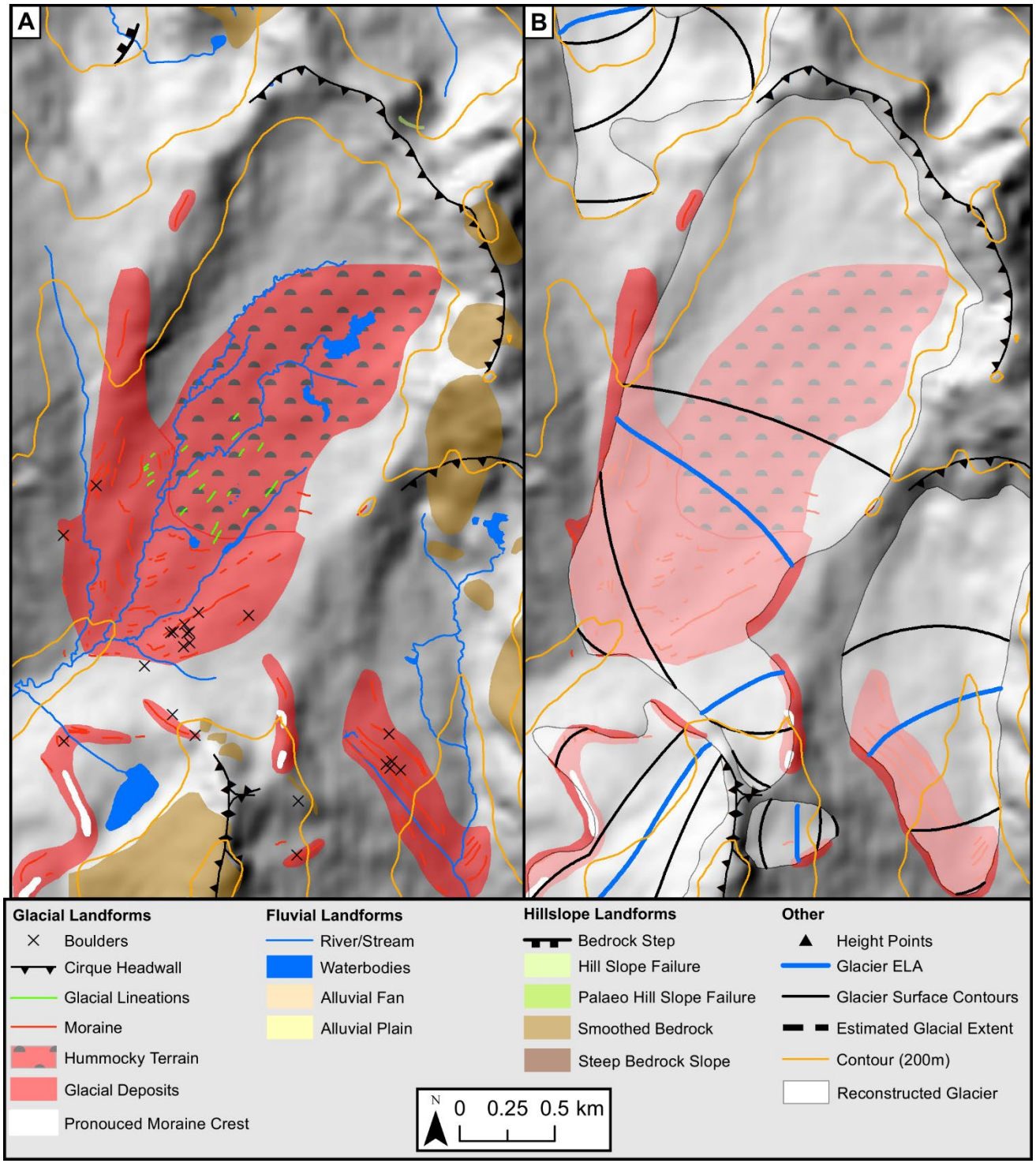

Supplementary Figure 7. Zoom in of Redondo de Zapalache 2 glacier valley within the southeastern glacier zone, corresponding with Figure 9 B subset 1 with A) mapped geomorphology and B) the subsequent reconstructed glacier LLGM extent. Base map is a hillshade from the ALOS 30 m DEM.

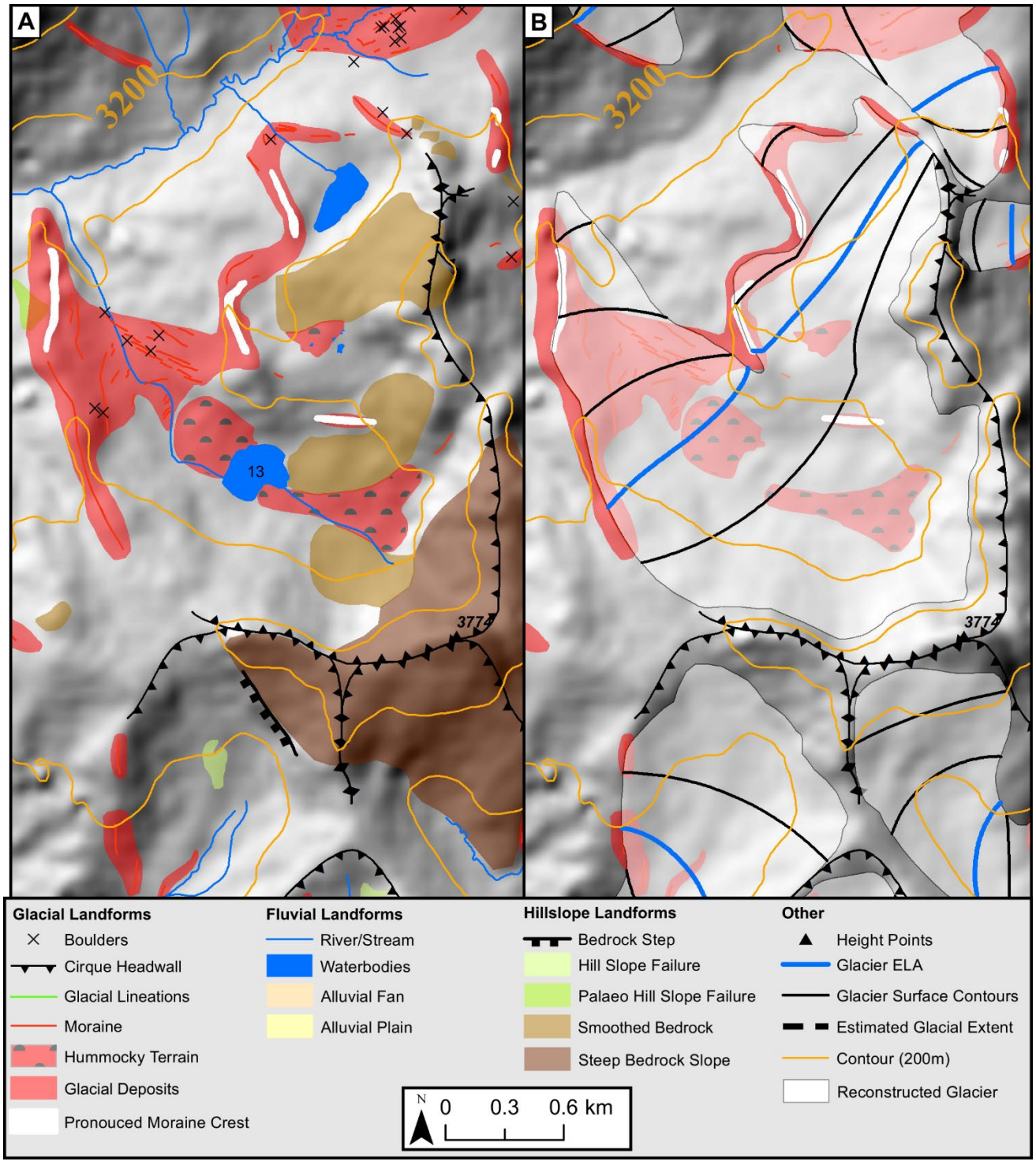

Supplementary Figure 8. Zoom in of Redondo de Zapalache 1 glacier valley within the southeaster glacier zone, corresponding with Figure 9 A subset 2 with A) mapped geomorphology and B) the subsequent reconstructed glacier LLGM extent. Base map is a hillshade from the ALOS 30 m DEM.

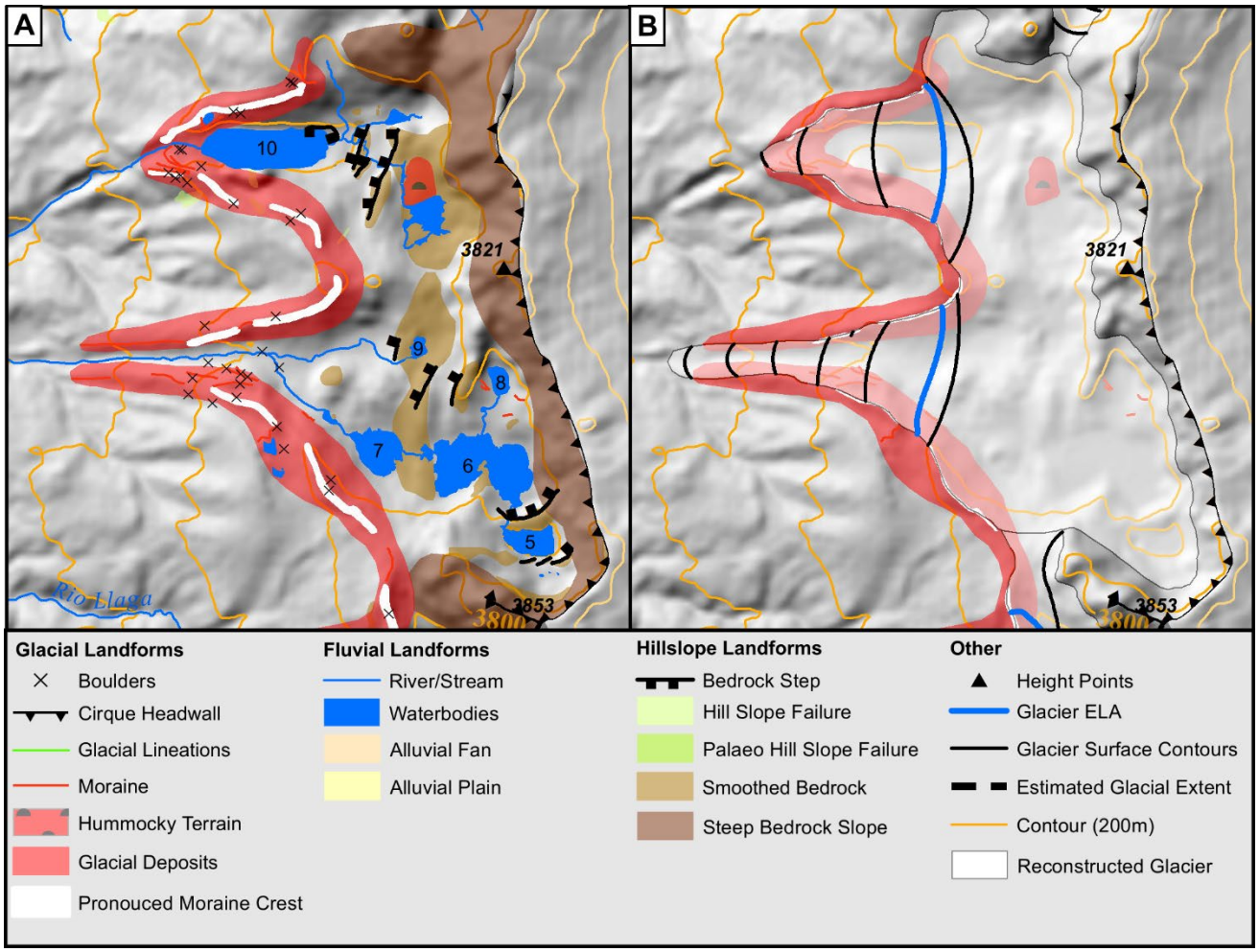

Supplementary Figure 9. Zoom in of the Arrebiatadas Glacier within the western glacier cirques zone, corresponding with Figure 10 B subset 1 with A) mapped geomorphology and B) the subsequent reconstructed glacier LLGM extent. Base map is a hillshade from the ALOS 30 m DEM.

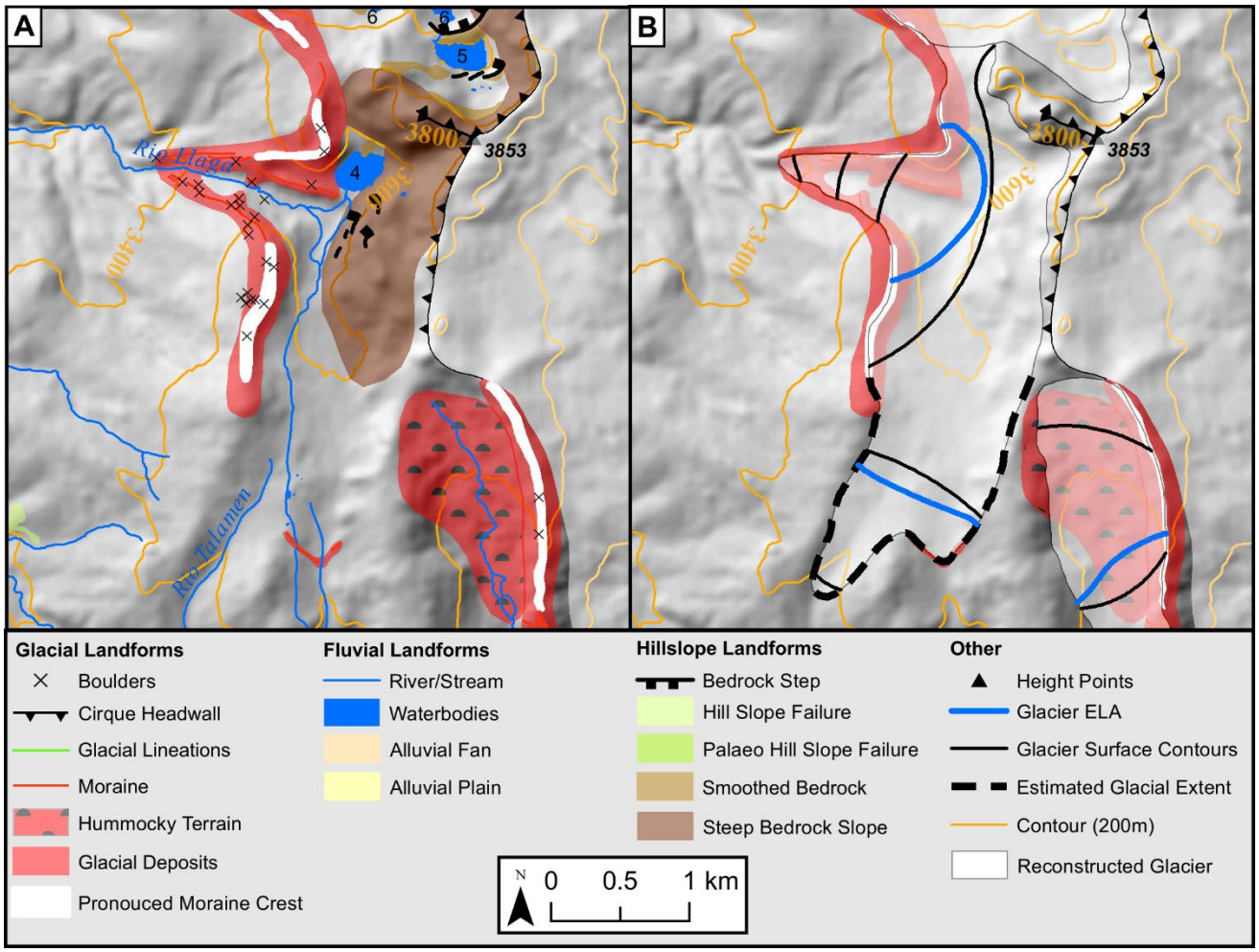

Supplementary Figure 10. Zoom in of the el Ray Inca Glacier within the western glacier cirques zone, corresponding with Figure 10 B subset 2 with A) mapped geomorphology and B) the subsequent reconstructed glacier LLGM extent. Base map is a hillshade from the ALOS 30 m DEM.

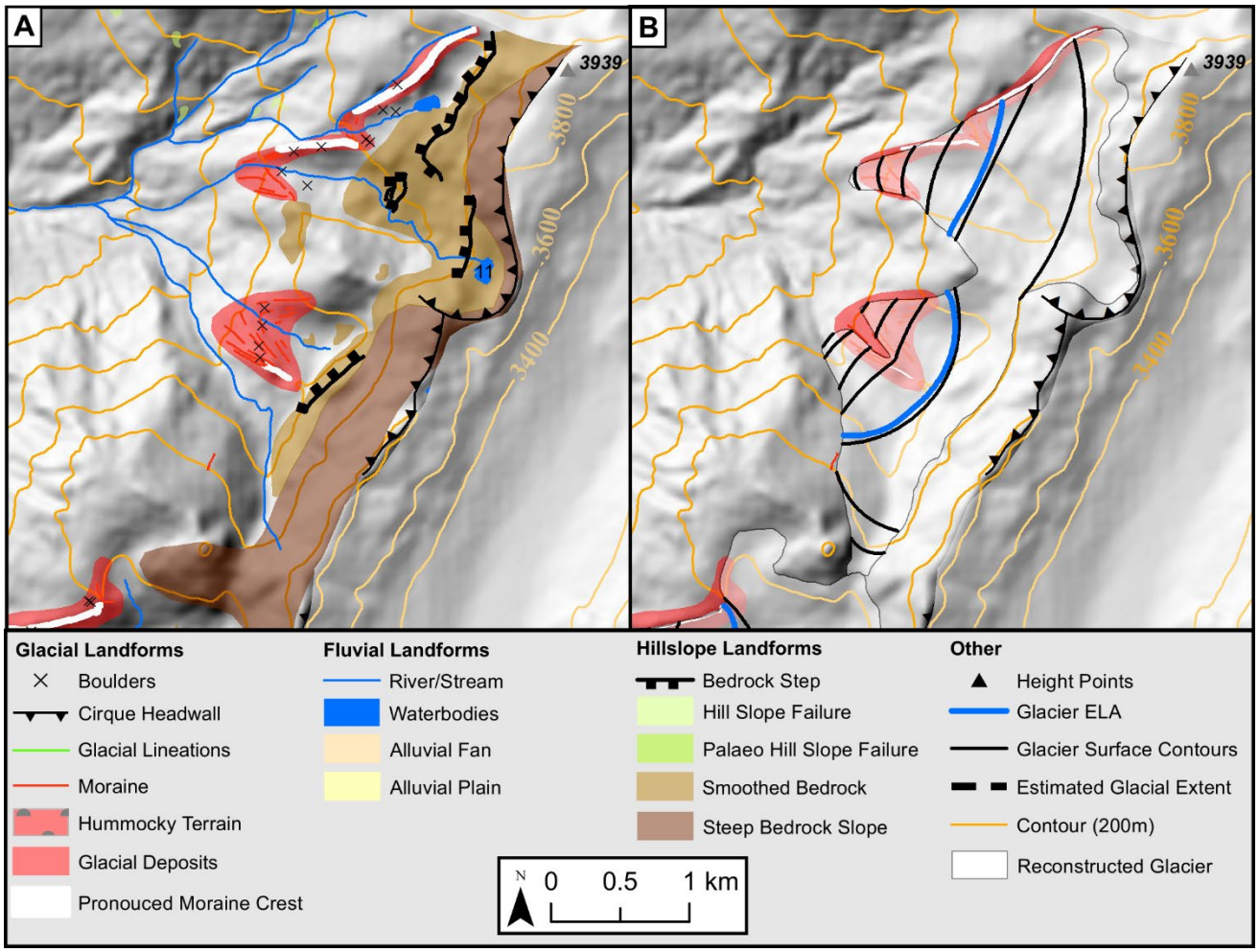

Supplementary Figure 11. Zoom in of the Negra glacier within the western glacier cirques zone, corresponding with Figure 10 B subset 3 with A) mapped geomorphology and B) the subsequent reconstructed glacier LLGM extent. Base map is a hillshade from the ALOS 30 m DEM.

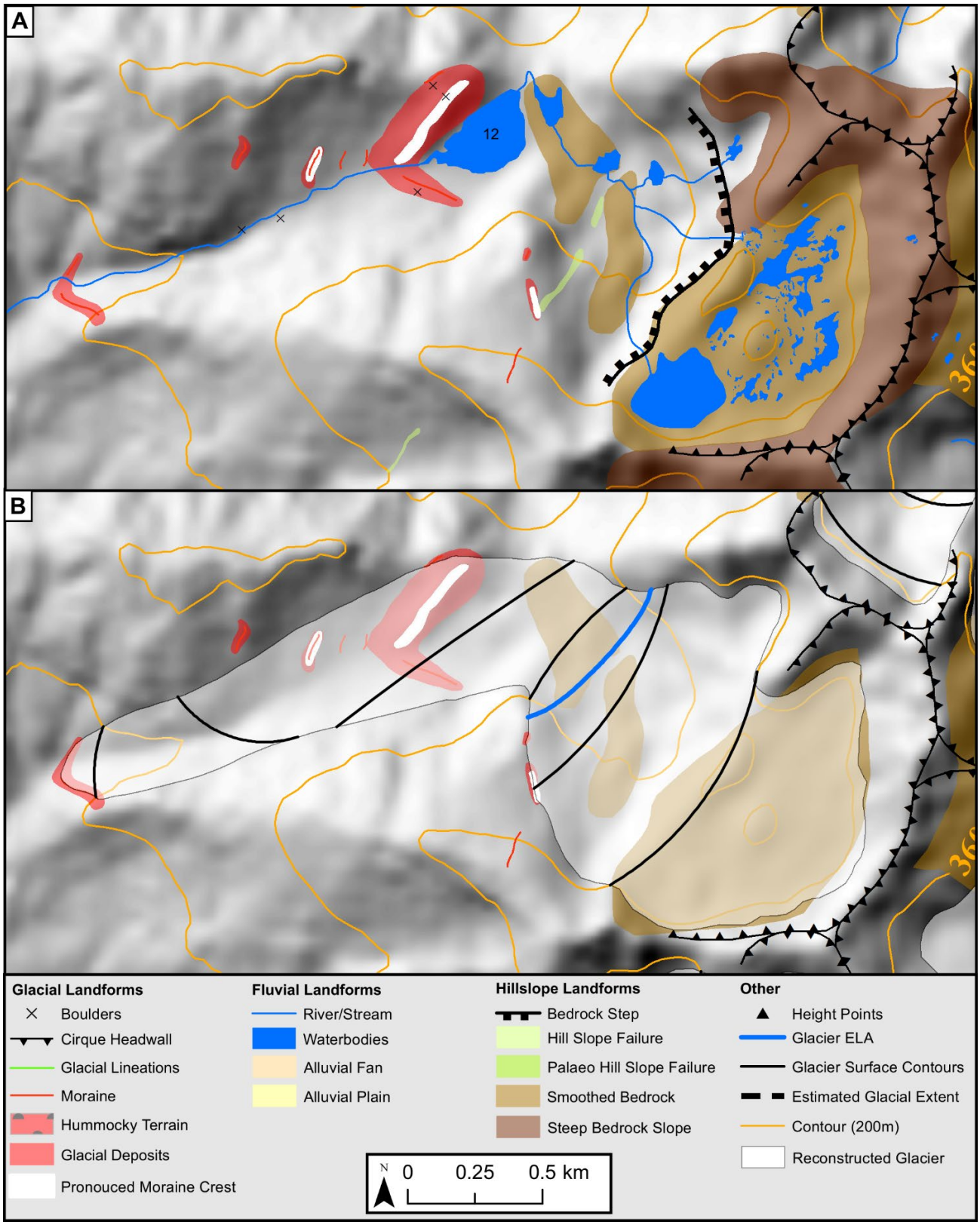

Supplementary Figure 12. Zoom in of the Pablo glacier # within the northern glacier valleys zone, corresponding with Figure 11 A subset 1 with A) mapped geomorphology and B) the subsequent reconstructed glacier LLGM extent. Base map is a hillshade from the ALOS 30 m DEM.

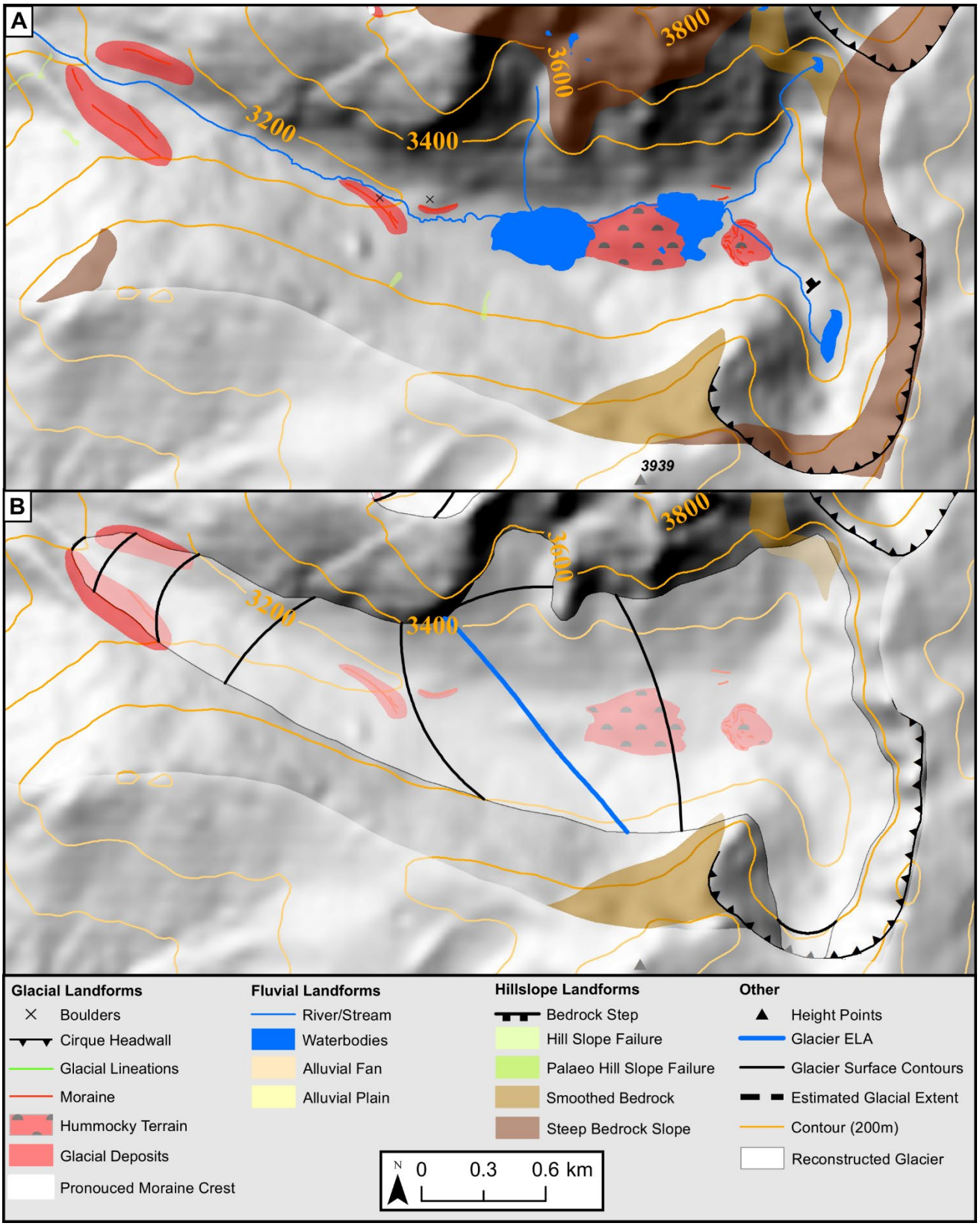

Supplementary Figure 13. Zoom in of the Pablo glacier # within the northern glacier valleys zone, corresponding with Figure 11 B subset 2 with A) mapped geomorphology and B) the subsequent reconstructed glacier LLGM extent. Base map is a hillshade from the ALOS 30 m DEM.

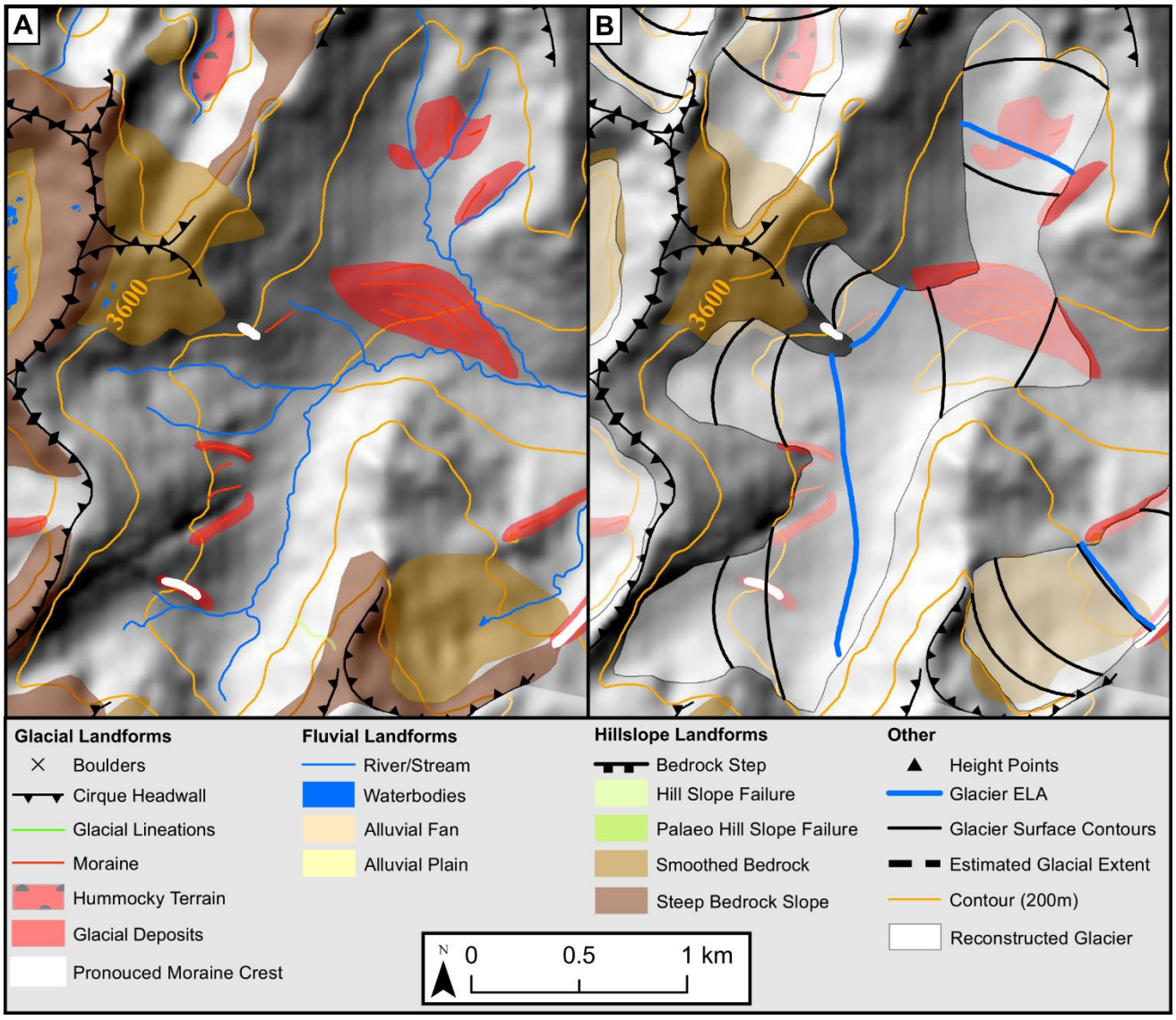

Supplementary Figure 14. Zoom in of the Pablo glacier # within the northern glacier valleys zone, corresponding with Figure 11 B subset 3 with A) mapped geomorphology and B) the subsequent reconstructed glacier LLGM extent. Base map is a hillshade from the ALOS 30 m DEM.

Supplementary Table 2. Studies within the northern Tropical Andes that determine temperature change (ΔT) ordered from the most northern latitude to the most southern

Location	Method	ΔELA (m)	ΔT (°C)	Reference
Merida Andes, Venezuelan	AAR (0.66-0.87); AABR (5, 10, 15) + EMBE/ATLR	-850-1420	-8.8 ± 2.0 -6.4 ± 1	Stansell et al. (2007)
Bogotá, Colombia	*	-1217	-7.9	Mark et al. (2005)
Bogotá, Columbia	AABR (1.0, 5.0, 7.0) + ATLR	-1300	-6-8	Mark and Helmens (2005)
Huascarán, Peru	Ice Core	NA	-8	Thompson et al. (1995)
Cordillera Blanca and Oriental, Peru	THAR + ATLR	~-1000	-5-6	Rodbell (1992)
Cordillera Blanca, Peru	*	-1058	-6.1	Mark et al. (2005)
Southern Andes (8-22°S)	AAR (0.6) + ATLR	-900 ± 135	-5–6.4	Porter (2001)
Junin Valleys, Peru Milluni Valley, Bolivia	THAR (0.4) + ATRL	-300-600	-2-4	Smith et al. (2005)
Junin Plain, Peru	THAR (0.45); AAR (0.65); AABR (0.65, 0.7) + ATLR	-220-550	-2.5 ± 1	Ramage et al. (2005)
Nevado Coropuna, Peru	MELM + ATLR	-550-770	~-4.5-5.2	Bromley et al. (2011)
Nevado Coropuna, Peru	AABR (1, 1.5, 2, 2.5, 3) + ATLR	-991	-6.4	Úbeda et al. (2018)
Central Andes	*	-804	-7.2	Mark et al. (2005)
Sajama, Bolivia	Ice Corp	NA	-5	Thompson et al. (1998)

AAR = Accumulation-Area Ratio
AABR = Area-Altitude Balance Ratio
MELM = Maximum Elevation of Lateral Moraines
THAR = Toe-to-Headwall Altitude Ratio
CF = Cirque-floor Altitude
ATLR = Air Temperature Lapse Rate
EMBE = Energy Mass-Balance Equation

*Mark et al. (2005) combines a number of studies in their results thus no method is reported

References

Bromley, G.R.M., Hall, B.L., Rademaker, K.M., Todd, C.E., and Racovteanu, A.E. (2011). Late Pleistocene snowline fluctuations at Nevado Coropuna (15°S), southern Peruvian Andes. *Journal of Quaternary Science* 26(3)**,** 305-317. doi: 10.1002/jqs.1455.

[Dataset] Lee, E., Ross, N., Henderson, A.C.G., Russell, A.J., Jamieson, S.S.R., and Fabel, D. (2022). *Mapped geomorphological features and reconstructed glaciers within the Lagunas de las Huaringas, Peru.* doi: https://doi.org/10.25405/data.ncl.19307591.v1.

Mark, B.G., Harrison, S.P., Spessa, A., New, M., Evans, D.J.A., and Helmens, K.F. (2005). Tropical snowline changes at the last glacial maximum: A global assessment. *Quaternary International* 138-139**,** 168-201. doi: https://doi.org/10.1016/j.quaint.2005.02.012.

Mark, B.G., and Helmens, K.F. (2005). Reconstruction of glacier equilibrium-line altitudes for the Last Glacial Maximum on the High Plain of Bogotá, Eastern Cordillera, Colombia: climatic and topographic implications. *Journal of Quaternary Science* 20(7-8)**,** 789-800. doi: 10.1002/jqs.974.

Porter, S.C. (2001). Snowline depression in the tropics during the Last Glaciation. *Quaternary Science Reviews* 20(10)**,** 1067-1091. doi: https://doi.org/10.1016/S0277-3791(00)00178-5.

Ramage, J.M., Smith, J.A., Rodbell, D.T., and Seltzer, G.O. (2005). Comparing reconstructed Pleistocene equilibrium-line altitudes in the tropical Andes of central Peru. *Journal of Quaternary Science* 20(7-8)**,** 777-788. doi: 10.1002/jqs.982.

Rodbell, D. (1992). Late Pleistocene equilibrium-line reconstructions in the northern Peruvian Andes. *Boreas* 21(1)**,** 43-52. doi: 10.1111/j.1502-3885.1992.tb00012.x.

Smith, J.A., Seltzer, G.O., Farber, D.L., Rodbell, D.T., and Finkel, R.C. (2005). Early Local Last Glacial Maximum in the Tropical Andes. *Science* 308(5722)**,** 678 - 681. doi: 10.1126/science.1107075.

Stansell, N.D., Polissar, P.J., and Abbott, M.B. (2007). Last glacial maximum equilibrium-line altitude and paleo-temperature reconstructions for the Cordillera de Mérida, Venezuelan Andes. *Quaternary Research* 67(1)**,** 115-127. doi: https://doi.org/10.1016/j.yqres.2006.07.005.

Thompson, L.G., Davis, M.E., Mosley-Thompson, E., Sowers, T.A., Henderson, K.A., Zagorodnov, V.S., et al. (1998). A 25,000-Year Tropical Climate History from Bolivian Ice Cores. *Science* 282(5395)**,** 1858-1864. doi: 10.1126/science.282.5395.1858.

Thompson, L.G., Mosley-Thompson, E., Davis, M.E., Lin, P.N., Henderson, K.A., Cole-Dai, J., et al. (1995). Late glacial stage and holocene tropical ice core records from Huascarán, Peru. *Science* 269(5220)**,** 46-50. doi: 10.1126/science.269.5220.46.

Úbeda, J., Bonshoms, M., Iparraguirre, J., Sáez, L., De la Fuente, R., Janssen, L., et al. (2018). Prospecting Glacial Ages and Paleoclimatic Reconstructions Northeastward of Nevado Coropuna (16° S, 73° W, 6377 m), Arid Tropical Andes. *Geosciences* 8(8)**,** 307. doi: https://doi.org/10.3390/geosciences8080307.